

# Micro-Raman evidence for topological charge order across the superconducting dome of $\text{La}_{2-x}\text{Sr}_x\text{CuO}_4$

D. Lampakis and E. Liarokapis

*Department of Physics, National Technical University, GR-15780 Athens, Greece*

C. Panagopoulos

*Cavendish Laboratory and IRC in Superconductivity, University of Cambridge, Madingley Road, CB3 0HE, United Kingdom*

(Received 28 January 2006; published 19 May 2006)

The doping dependence of the micro-Raman spectra of high-quality  $\text{La}_{2-x}\text{Sr}_x\text{CuO}_4$  microcrystals with  $x = 0.0\text{--}0.45$  has been investigated in the region 10–300 K. The phonon at  $\sim 100\text{ cm}^{-1}$  of the orthorhombic phase shows a classical soft-mode behavior up to  $x=0.17$ , supporting its correlation with the low-temperature orthorhombic to high-temperature tetragonal transition. In the  $xx$ - $yy$  polarization spectra of the superconducting concentrations new modes at  $\sim 150$  and  $370\text{ cm}^{-1}$  related to the symmetry breaking and a broad band at  $\sim 280\text{ cm}^{-1}$  are attributed to the charge ordering at temperatures well above  $T_c$ . At all temperatures studied a correlation has been found between the doping dependence of the transition temperature and the intensity of the bands at  $\sim 150$ ,  $\sim 280$ , and  $\sim 370\text{ cm}^{-1}$ , the intensity of the La/Sr mode, and the asymmetry of the apex phonon.

DOI: [10.1103/PhysRevB.73.174518](https://doi.org/10.1103/PhysRevB.73.174518)

PACS number(s): 74.72.-h, 78.30.-j, 63.20.-e

## INTRODUCTION

It is known that the  $\text{La}_{2-x}\text{Sr}_x\text{CuO}_4$  (LSCO) superconductor shows a variety of phases with doping and temperature.<sup>1</sup> One of the main conclusions from Raman investigations of the vibrational modes of  $\text{La}_2\text{CuO}_4$  has been the existence of a soft mode at  $\sim 100\text{ cm}^{-1}$  (12 meV) of  $A_g$  symmetry, attributed to tilting vibrations of the  $\text{CuO}_6$  octahedra about the diagonal (110) axis.<sup>2–4</sup> This mode has been correlated with the observed high-temperature tetragonal (HTT) to low-temperature orthorhombic (LTO) structural phase transition of LSCO (Ref. 5) and has been studied for Sr-doped samples, up to  $x=0.07$ .<sup>2,3,6</sup> As the structural critical temperature decreases with increasing Sr content,<sup>1</sup> the soft mode can only be observed at LT and it has not been studied for  $x > 0.07$ . Here we examine the behavior of the soft mode for even higher Sr concentrations and, particularly, for  $x$  values near optimum.

The two strong modes of this compound are of  $A_g$  symmetry and have been attributed to the vibrations of the La/Sr and the apex oxygen ( $\text{O}_z$ ) atoms along the  $c$  axis. Their dependence on temperature has been studied for a wide range of Sr doping. Our studies of these materials at room temperature (RT) have shown that the asymmetry of the apex phonon and the relative intensity of the La/Sr phonon over the apex mode show a maximum for the Sr concentrations at which the compound appears with the maximum transition temperature to superconductivity.<sup>6</sup> It was concluded that, since this effect cannot be assigned to any apparent structural changes of the system, it might originate from a charge redistribution, which occurs at temperatures well above  $T_c$  and affects the electronic states and the polarizabilities of the La/Sr and apex atoms at some critical Sr concentration. For this reason, it was interesting to examine how this correlation of some phonon characteristics with the transition temperature evolves at low temperatures.

Furthermore, we found that, with increasing  $x$  two symmetry-forbidden broad modes at  $\sim 150$  and  $\sim 370\text{ cm}^{-1}$

appear in the  $xx$ - $yy$  polarization Raman spectra, despite the phase transition from the orthorhombic to the more symmetric tetragonal phase.<sup>2,3</sup> In the low-temperature spectra a broadband at  $\sim 280\text{ cm}^{-1}$  has been also observed.<sup>2</sup> A common feature of these peaks is that their intensity shows a maximum for the optimally doped samples.<sup>6</sup> In this work we have investigated the temperature dependence of the Raman spectra for various Sr contents and compare with previously reported room-temperature data.

## EXPERIMENTAL SETUP

Individual microcrystallites from a selected series of high-quality  $\text{La}_{2-x}\text{Sr}_x\text{CuO}_4$  polycrystalline compounds, with Sr doping in the range  $0.00 \leq x \leq 0.45$ , have been studied in the 10–300-K temperature region. The carefully prepared samples have been characterized as described elsewhere.<sup>6</sup> The Raman spectra were obtained in the approximate  $y(zz)\bar{y}$  and  $y(xx)\bar{y}$  [or  $x(yy)\bar{x}$ ] scattering configurations or a mixture of them (as the  $x$  and  $y$  axes could not be discriminated in the twinned samples) at nominal temperatures from 10 K to RT with a Jobin-Yvon T64000 triple spectrometer, equipped with a liquid-nitrogen-cooled charge-coupled-device (CCD) and a microscope (100 $\times$  magnification). Low temperatures were achieved by using an open-cycle Oxford cryostat operating with liquid nitrogen or with liquid helium. The 514.5-nm wavelength of an  $\text{Ar}^+$  laser was used for excitation at a power level of  $\leq 0.1\text{ mW}/\mu\text{m}^2$ . The local sample heating due to the laser beam was estimated to be less than 10 K. Accumulation times were of the order of 4–5 h, and usually two microcrystallites have been studied for each strontium concentration (i.e.,  $x=0.00, 0.03, 0.05, 0.07, 0.092, 0.125, 0.17, 0.20$ , and  $0.24$ ).

## RESULTS

Typical spectra for selected doping and temperatures in the  $y(zz)\bar{y}$  and  $y(xx)\bar{y}$  [or  $x(yy)\bar{x}$ ] polarization, are shown in

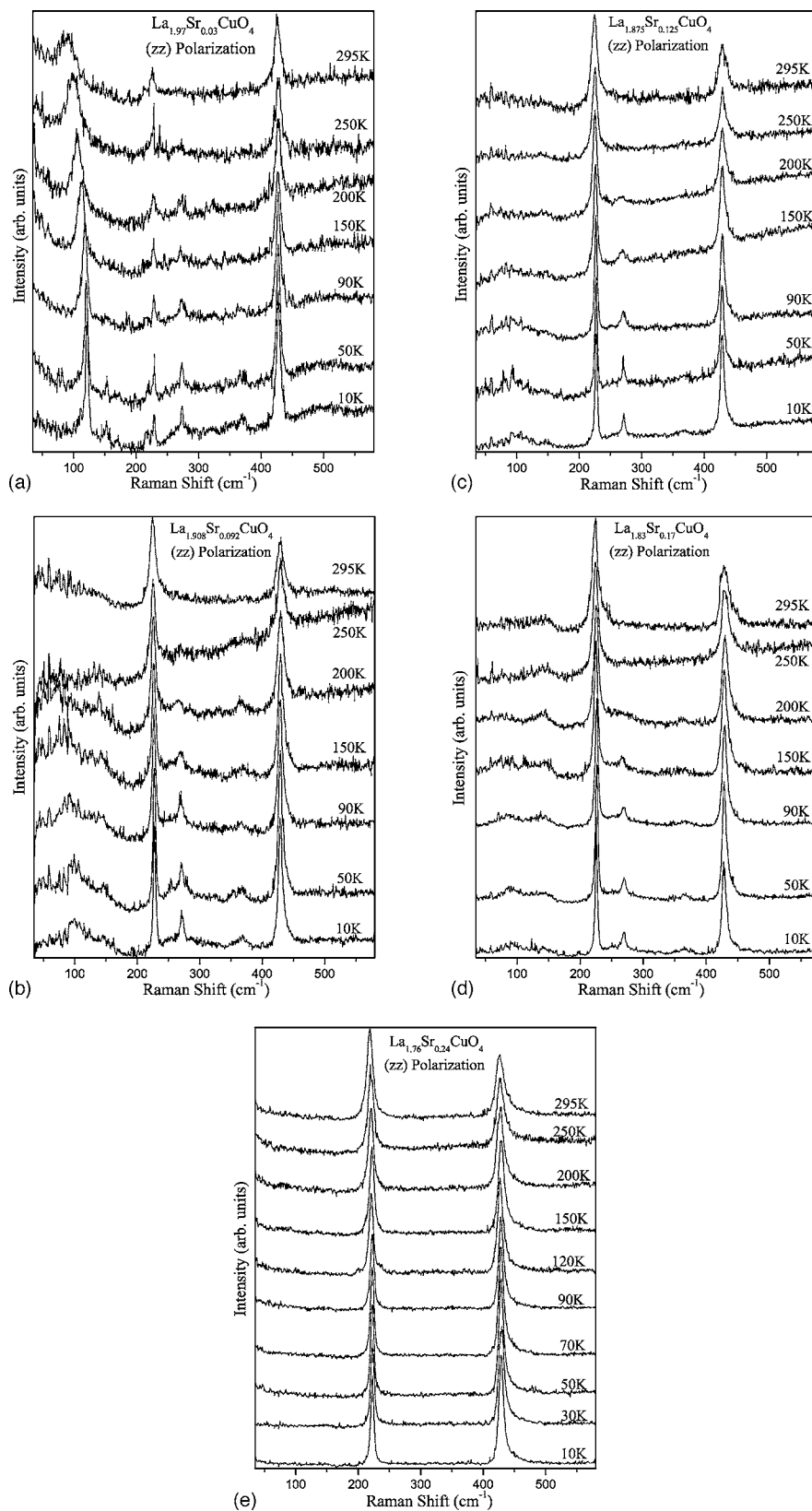


FIG. 1. Typical Raman spectra for selected temperatures for the  $x=0.03$  (a),  $x=0.092$  (b),  $x=0.125$  (c),  $x=0.17$  (d), and  $x=0.24$  (e) samples in the  $y(zz)y$  scattering geometry using the 514.5-nm excitation wavelength.

Figs. 1 and 2, respectively. In all cases, the two strong La/Sr and apex oxygen phonons of  $A_g$  symmetry appear. According to the  $\text{La}_{2-x}\text{Sr}_x\text{CuO}_4$  phase diagram, the structural critical transition temperature  $T_{ot}$ , for the insulating  $\text{La}_{1.97}\text{Sr}_{0.03}\text{CuO}_4$  sample is  $\sim 560$  K.<sup>1</sup> Thus, this compound remains ortho-

rhombic throughout the temperature range studied and the soft mode appears in the low-energy part of the  $zz$  polarization spectra for all temperatures [Fig. 1(a)]. The mode at  $\sim 270$   $\text{cm}^{-1}$  attributed to the vibrations of the plane oxygens along the  $c$  axis is observed in all  $zz$  spectra of Fig. 1(a). This

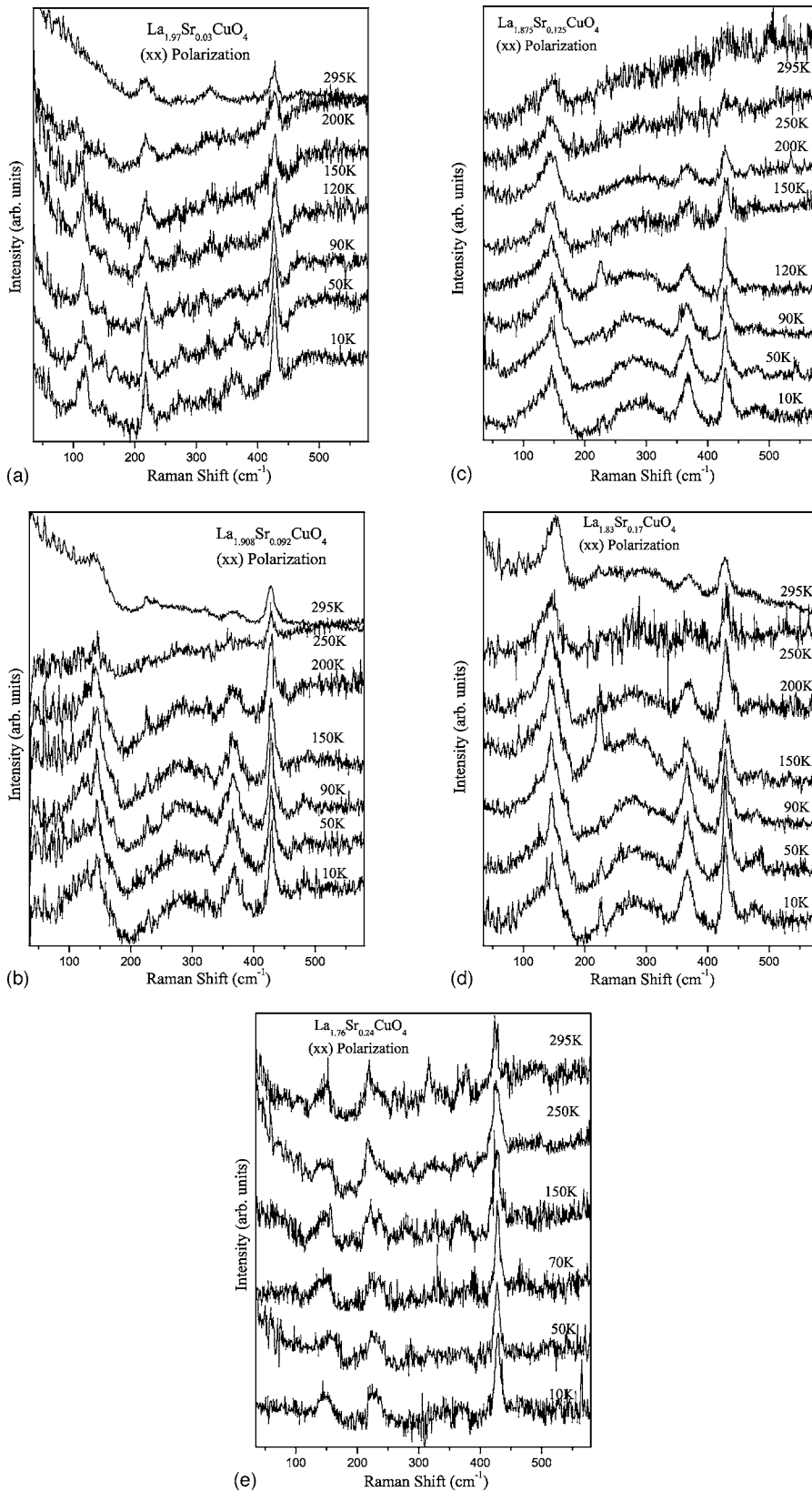


FIG. 2. Typical Raman spectra for selected temperatures for the  $x=0.03$  (a),  $x=0.092$  (b),  $x=0.125$  (c),  $x=0.17$  (d), and  $x=0.24$  (e) samples in the  $y(xx)\bar{y}$  [or  $x(yy)\bar{x}$ ] scattering geometry using the 514.5-nm excitation wavelength.

phonon is also correlated with the HTT $\rightarrow$ LTO structural phase transition since the vibrations of the plane oxygens are not Raman active in the tetragonal phase.<sup>2,3,7</sup> Concerning the  $xx$ - $yy$  polarization spectra for the  $x=0.03$  sample [Fig. 2(a)], new bands at  $\sim 150$  and  $370$   $\text{cm}^{-1}$  are observed for tempera-

tures below  $\sim 100$  K. These broad peaks are weakly observed at the same low temperatures in the  $zz$  polarization spectra [Fig. 1(a)]. With increasing doping these two bands appear at much higher temperatures, even at RT in the spectra of the superconducting materials [tetragonal phase, Figs.

2(b)–2(e)]. Therefore, their appearance cannot be related with the  $\text{HTT} \rightarrow \text{LTO}$  structural phase transition. Besides, a weak mode at  $\sim 320 \text{ cm}^{-1}$  of  $A_{1g}$  symmetry<sup>3</sup> is present in the  $xx$ - $yy$  spectra with energy independent of temperature [Fig. 2(a)]. A broad continuum around  $280 \text{ cm}^{-1}$  is also present at low temperatures and for intermediate doping in the same polarization spectra [Figs. 2(c) and 2(d)]. Finally, the mode at  $\sim 100 \text{ cm}^{-1}$  rapidly softening with increasing temperature [Fig. 2(a)] is apparently an escape from the  $zz$  polarization.

In the  $zz$  polarization spectra of the underdoped superconductor  $\text{La}_{1.908}\text{Sr}_{0.092}\text{CuO}_4$  with  $T_{ot} \sim 300 \text{ K}$ , the modes at  $\sim 100$  and  $270 \text{ cm}^{-1}$  are observed only below  $250 \text{ K}$  [Fig. 1(b)]. For  $T > 250 \text{ K}$  they are not detectable due to the small tilting of the octahedra, in agreement with their relation to the orthorhombic deformation of the cell. The weak peaks at  $\sim 150 \text{ cm}^{-1}$  and  $\sim 365 \text{ cm}^{-1}$  must be the same modes with the  $xx$ - $yy$  polarization spectra [see Fig. 2(b)]. The very broad band at  $\sim 280 \text{ cm}^{-1}$  observed in  $xx$ - $yy$  polarization at low temperatures with increasing intensity should not be confused with the narrow peak at  $\sim 270 \text{ cm}^{-1}$  of the plane oxygen atoms that appears in the  $zz$  polarization spectra. The intensity increment of the three bands at  $\sim 150$ ,  $\sim 280$ , and  $\sim 370 \text{ cm}^{-1}$  with decreasing temperature becomes more obvious in the samples with  $x=0.125$  and  $0.17$  [Figs. 2(c) and 2(d)]. In  $\text{La}_{1.76}\text{Sr}_{0.24}\text{CuO}_4$  the intensity of the three broadbands appears substantially reduced [Fig. 2(e)]. This indicates a doping dependence of these bands and, possibly, small lattice distortions induced by the variation of the Sr content. The dependence of these bands on temperature and Sr concentration is examined below.

For the  $x=0.125$  compound, some traces of the soft mode can be detected in the  $zz$  spectrum at  $250 \text{ K}$  with increasing intensity at lower temperatures [Fig. 1(c)]. Concerning the  $x=0.17$  sample the soft mode starts appearing in the  $zz$  spectra at even lower temperatures [Fig. 1(d)], in agreement with the phase diagram, where no tilting is expected in the tetragonal phase above  $150 \text{ K}$ .<sup>1</sup> The soft mode has not been detected in the  $zz$  spectra for any temperature in the overdoped superconductor  $\text{La}_{1.76}\text{Sr}_{0.24}\text{CuO}_4$  [Fig. 1(e)] and for  $x=0.20$  as expected, since the compound remains tetragonal at any temperature.<sup>1</sup>

The soft-mode behavior of the low-energy  $A_g$  mode at  $\sim 100 \text{ cm}^{-1}$  has already been shown for low Sr concentrations, up to  $x=0.07$ .<sup>2,3,6</sup> In Fig. 3(a) the temperature dependence of the energy of this mode for selected concentrations is presented. The values of the energy were determined by fitting the low-energy part of the Raman spectra with Lorentzian curves. In Fig. 3(a), the solid lines are best fit to the data with curves  $\omega_{soft} \propto (T_{ot} - T)^{1/2}$ , which assume a second-order phase transition. For most concentrations the zero phonon energy occurs close to the structural critical temperature of each concentration. But for the  $x=0.17$  sample, the soft-mode energy tends to zero at temperature fairly larger than  $T_{ot}$ . This discrepancy may originate from the fact that the soft-mode peak for this sample is very weak for all temperatures studied, and, therefore, the accurate determination of the energy was very difficult. Figure 3(b) shows the temperature dependence of the linewidth of the soft mode, for the  $x=0.092$ – $0.17$  samples. In each case, on approaching the  $T_{ot}$  the width increases as in a second-order phase transition.

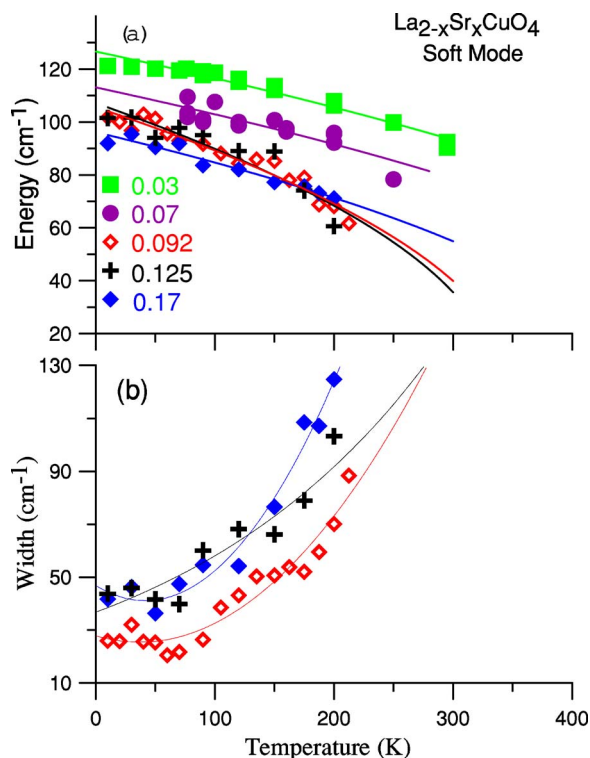


FIG. 3. (Color online) Dependence of the energy (a) and the linewidth (b) on temperature for the soft phonon observed in  $y(zz)\bar{y}$  scattering geometry spectra for the  $x=0.03, 0.092, 0.125,$  and  $0.17$  samples.

Also, it should be noticed that the soft mode is very weak for temperatures above  $200 \text{ K}$  for the  $x=0.092, 0.125,$  and  $0.17$  samples [Figs. 1(b)–1(d)], and, therefore, the fitting results above this temperature are not taken into account in graphs of Fig. 3. The above results support the correlation of this mode with the structural phase transition  $\text{HTT} \rightarrow \text{LTO}$ . As seen in Fig. 4, the energy of the soft mode decreases with increasing Sr content while its width increases as expected from the reduced tilting of the octahedra with increasing doping.

As mentioned, the mode at  $\sim 270 \text{ cm}^{-1}$  observed in the  $zz$  scattering polarization is attributed to the vibrations of the plane oxygen atoms along the  $c$  axis of  $A_g$  symmetry. It is correlated with the structural phase transition, since it appears only in the spectra of the orthorhombic phase of the compound, just like the soft mode. In particular, for the insulating samples [Fig. 1(a) for  $x=0.03$ ] this mode appears in the whole temperature range  $10$ – $300 \text{ K}$ , while, for the doped  $x=0.092$  and  $0.125$  samples, it can only be seen at temperatures below  $250 \text{ K}$ . For the optimally doped  $x=0.17$  sample, the appearance of this mode at temperatures above  $150 \text{ K}$  (which is the nominal  $T_{ot}$  for this compound), just like the soft mode, supports the assumption of the existence of tilted octahedra at this concentration and, thus, the  $T_{ot}$  for this sample should be considered  $\sim 200 \text{ K}$ . For the overdoped samples this mode has not been detected in all temperatures studied. Although the weakness of this mode and the existence of the strong La/Sr phonon close to it make difficult the accurate determination of the mode energy and width, it

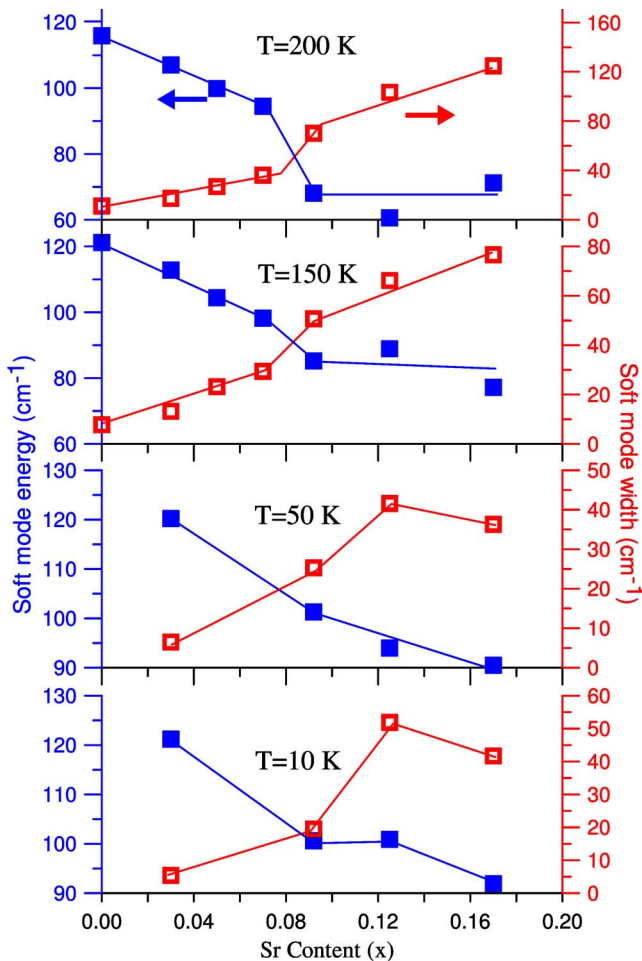


FIG. 4. (Color online) The dependence of the soft phonon energy and linewidth on doping at various temperatures.

can be clearly seen that there is an almost linear increase in energy with decreasing temperature of the order  $\sim 5\text{--}6\text{ cm}^{-1}$  (Fig. 1). This result is in disagreement with previously reported data where no energy shift with temperature has been observed for this mode.<sup>2,3</sup> In addition, it should be clarified that, although the appearance of this mode is correlated with the LTO  $\rightarrow$  HTT transition, it does not show a classical soft-mode behavior; i.e., its energy does not tend to zero near  $T_{ot}$  and its width does not show a significant broadening, similar to the broadening of the mode at  $\sim 100\text{ cm}^{-1}$ .

In Fig. 5(a) the variation of the energy of the La/Sr mode as a function of temperature for the  $x=0.092\text{--}0.24$  superconducting samples is presented. As seen, the phonon energy decreases almost linearly with temperature for each Sr content by approximately  $3\text{--}4\text{ cm}^{-1}$  in the range  $10\text{--}300\text{ K}$ . A similar behavior has also been detected for the insulating  $x=0.0$ ,  $x=0.03$  [also shown in Fig. 5(a)] and underdoped superconducting ( $x=0.05, 0.07$ ) compounds.<sup>6</sup> On the contrary, the apex energy remains practically constant with temperature for all compounds in the  $x=0.0\text{--}0.17$  range [Fig. 5(b) and Ref. 6]. Instead, there is a decrease of approximately  $3\text{ cm}^{-1}$ , with increasing temperature for the overdoped ( $x=0.24$ ) compound. It should be marked that for the optimally doped compounds ( $x=0.125$  and  $0.17$ ), the material under-

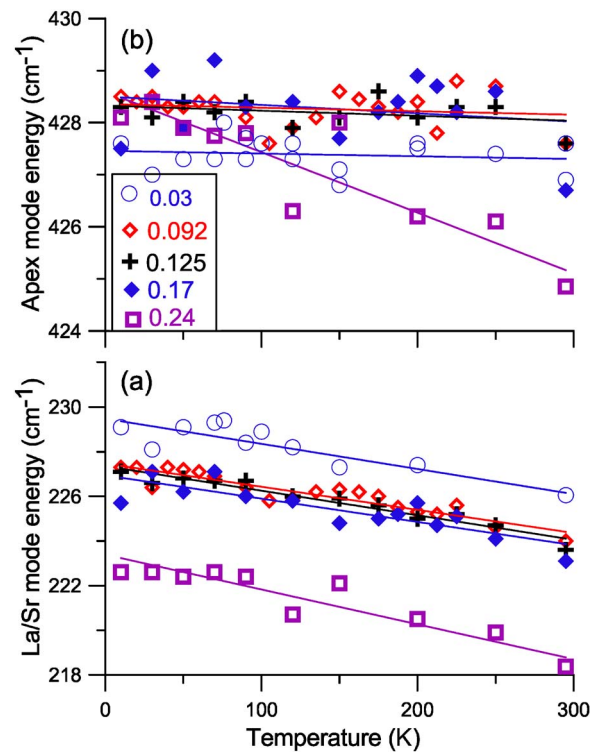


FIG. 5. (Color online) The dependence on temperature of the (a) La/Sr and (b) apex phonon energy for the  $x=0.03, 0.092, 0.125, 0.17,$  and  $0.24$  samples.

goes a structural phase transition HTT  $\rightarrow$  LTO phase in the temperature range studied. This transition is correlated to the tilting of the  $\text{CuO}_6$  octahedra about the (110) axis and apparently it does not affect the energy of the apex oxygen.

Figure 6 shows the linewidths of the La/Sr and apex oxygen modes with varying temperature for several doping levels. For all Sr concentrations the linewidth of both modes shows a typical anharmonic behavior increasing almost linearly with temperature above  $70\text{ K}$ . The total width increment is about  $8\text{ cm}^{-1}$ , for both phonons in all concentrations. The relative intensity of the two modes as a function of temperature is presented in Fig. 7 for the same concentrations. In a first approximation the relative intensity increases with temperature for all concentrations studied. But it appears that in the temperature range  $\sim 150\text{--}250\text{ K}$  there are some profound deviations from linearity for the samples around optimal doping. The maximum deviation is for the  $x=0.125$  compound; it is reduced for  $x=0.17$ , and it seems gradually to disappear for  $x=0.092$ , and  $x=0.24$ . *Since no structural modifications are expected at low temperatures for these compounds, this change perhaps involves other mechanisms and it is probably related to the plateau in the doping dependence of  $T_c$  and the charge ordering.*<sup>8</sup> It is also clear that the correlation observed at RT between this relative intensity and the variation of  $T_c$  with doping<sup>6</sup> remains at low temperatures.

Figure 8 shows the temperature dependence of the average energy and total apparent width of the wideband at  $\sim 150\text{ cm}^{-1}$ . At room temperature there is a band energy difference among the various concentrations, which diminishes at low temperatures. Besides, the temperature dependence of

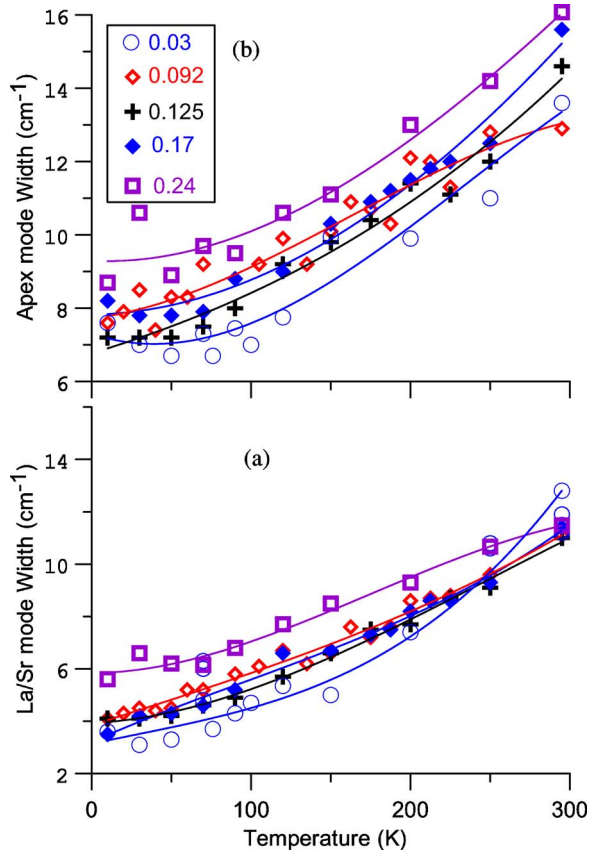


FIG. 6. (Color online) The dependence on temperature of the (a) La/Sr and (b) apex phonon linewidth for the  $x=0.03$ , 0.092, 0.125, 0.17, and 0.24 samples.

the band energy depends on the amount of doping. The bandwidth is almost independent of temperature for  $x \geq 0.20$ , while for lower doping levels it increases with decreasing temperature (Fig. 8). One can observe in Fig. 2 that this band

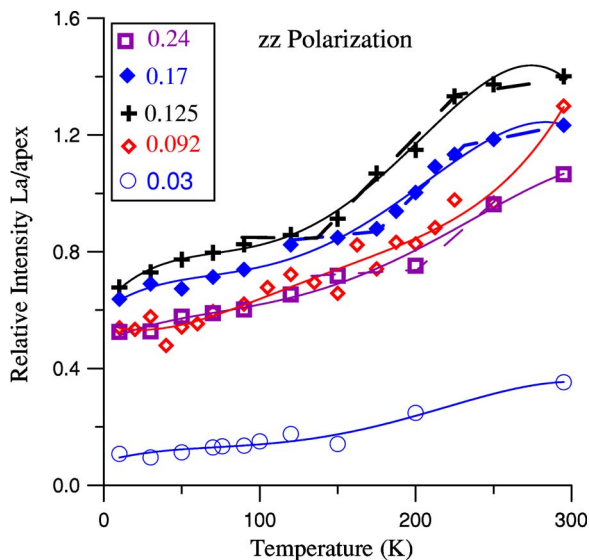


FIG. 7. (Color online) The relative intensity of the La/Sr phonon to the apex one as a function of temperature for the  $x=0.03$ , 0.092, 0.125, 0.17, and 0.24 samples.

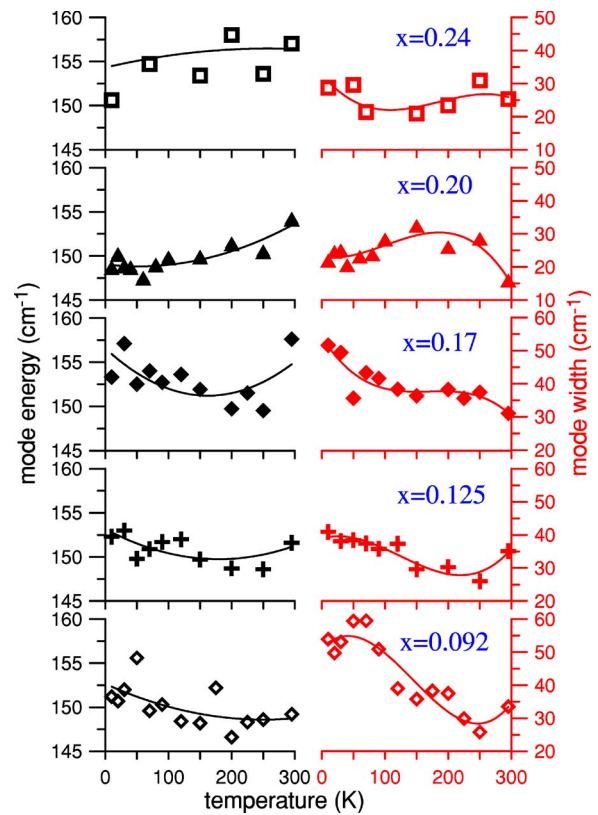


FIG. 8. (Color online) Energy and linewidth dependence on temperature for the mode at  $\sim 150$  cm<sup>-1</sup> observed in  $y(xx)\bar{y}$  scattering geometry spectra for  $x=0.092$ , 0.125, 0.17, 0.20, and 0.24.

for certain concentrations and below some temperature splits in two or three modes. Therefore, the modifications shown in Fig. 8 actually represent changes in the relative intensity and the width of those modes.

Figure 9 shows the temperature dependence of the energy and width of the symmetry forbidden mode at  $\sim 370$  cm<sup>-1</sup>. For the  $x=0.092$ –0.24 compounds the energy and width of the mode seem to be independent of doping and temperature. In the insulating sample ( $x=0.03$ ) a mode of similar energy appears in the  $xx$ - $yy$  spectra for temperatures below 100 K [Fig. 2(a)]. The energy of this mode depends strongly on temperature decreasing by  $\sim 8$  cm<sup>-1</sup> from  $T=90$  to 10 K. Its linewidth is initially narrow, but with decreasing temperature it increases reaching at 10 K almost the same value as for the  $x=0.092$ –0.24 samples [Fig. 9(b)].

The broadband at  $\sim 280$  cm<sup>-1</sup> appears mainly in the low-temperature  $xx$ - $yy$  spectra. At room temperature, traces of this band have been detected only for the  $x=0.17$  sample [Fig. 2(d)]. For  $x=0.092$  and 0.125 the band is observed for temperatures below 250 K [Figs. 2(b) and 2(c)], while for the  $x=0.03$  sample it seems not to be present to the lowest temperatures studied [Fig. 2(a)]. Similar to the  $\sim 150$  and 370-cm<sup>-1</sup> broad peaks, the appearance of this band cannot be correlated with Raman active modes or the  $\text{HTT} \rightarrow \text{LTO}$  phase transition. For  $x=0.125$  the transition temperature  $T_{ot}$  is nearly the same with the temperature at which the  $\sim 280$  cm<sup>-1</sup> band appears, but this is not the case for the  $x=0.092$  and  $x=0.17$  samples. Besides, the spectra of the  $x$

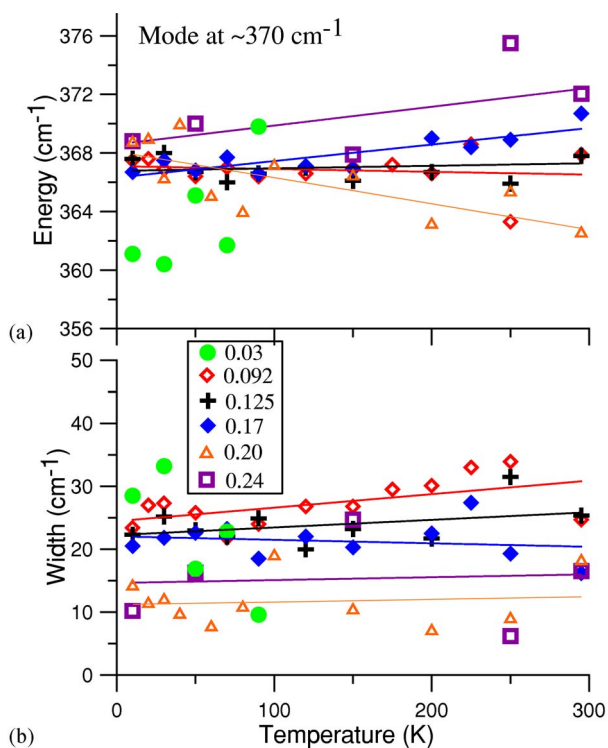


FIG. 9. (Color online) (a) Energy and (b) linewidth dependence on temperature for the mode at  $\sim 370$   $\text{cm}^{-1}$  observed in  $y(xx)\bar{y}$  scattering geometry spectra for  $x=0.03, 0.092, 0.125, 0.17, 0.20,$  and  $0.24$ .

$=0.03$  sample, which is orthorhombic even at room temperature, do not show this broadband. For the  $x=0.092$ – $0.17$  compounds, the energy of this band does not vary with temperature within experimental error [Fig. 10(a)], while its width appears to be very large ( $\sim 100$   $\text{cm}^{-1}$ ) and almost independent of temperature for all samples [Fig. 10(b)].

## DISCUSSION

The apex phonon energy shown in Fig. 5 (and from Ref. 6) remains practically unaffected with the variation of temperature for the  $x=0.03$ – $0.17$  samples and, only, for the overdoped  $x=0.24$  sample seems to decrease with increasing temperature ( $\sim 3$   $\text{cm}^{-1}$ ). This result for the  $x=0.03$ – $0.17$  compounds is in good agreement with the structural measurements, which have shown that the  $\text{Cu-O}_z$  bond is practically independent of temperature or varies by less than 0.2% for all doping levels.<sup>9</sup> For the overdoped  $x=0.24$  compound the disagreement for the overdoped region has also been observed at RT as a function of doping,<sup>6</sup> where the  $\text{Cu-O}_z$  bond decreases with increasing Sr concentration together with the energy of the apex oxygen mode.

Bianconi *et al.*<sup>8</sup> in an extended x-ray-absorption fine-structure (EXAFS) study has evaluated the  $\text{Cu-O}_{xy}$  and  $\text{Cu-O}_z$  bond lengths of the optimally doped  $\text{La}_{1.85}\text{Sr}_{0.15}\text{CuO}_4$  compound. They have shown that there are two  $\text{Cu-O}_z$  bond lengths that differ by  $0.08$ – $0.14$   $\text{\AA}$ , depending on the temperature of the material. Also, two different  $\text{Cu-O}_{xy}$  bonds have been observed for this material, but only for tempera-

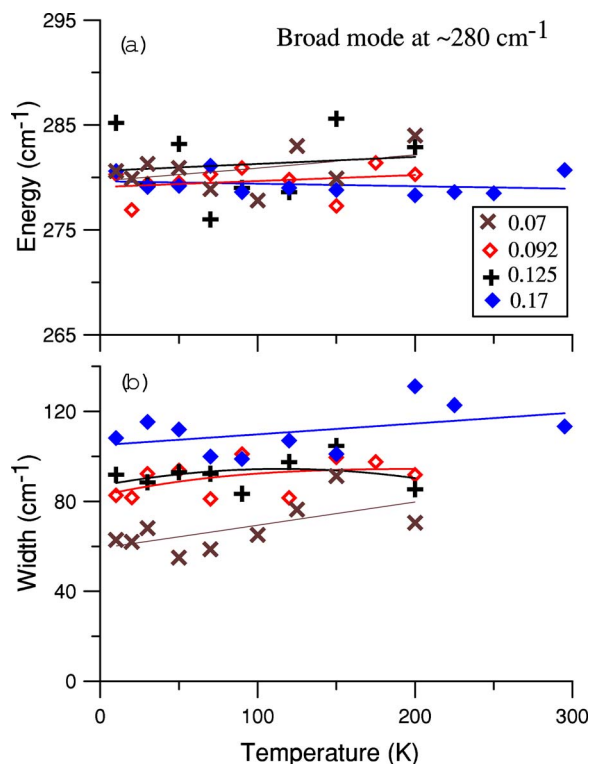


FIG. 10. (Color online) (a) Energy and (b) linewidth dependence on temperature for the mode at  $\sim 280$   $\text{cm}^{-1}$  observed in  $y(xx)\bar{y}$  scattering geometry spectra for the  $x=0.03, 0.092, 0.125,$  and  $0.17$  samples.

tures below 100 K (i.e., in the orthorhombic phase), whereas the tilting angle of the octahedra was found to be larger. From the above it was concluded that in the  $\text{La}_{1.85}\text{Sr}_{0.15}\text{CuO}_4$  structure apart of the normal (undistorted) there are also distorted octahedra. These local lattice distortions have been attributed to the existence of two types of stripes, the  $U$ -type, which is due to the undistorted octahedra, and the  $D$ -type which is due to the distorted ones.<sup>8</sup>

The existence of a shorter  $\text{Cu-O}_z$  bond would imply another weak phonon peak in the Raman spectra at the high-energy side of the band due to the vibrations of the apex oxygen atoms along the  $c$  axis ( $A_g$  symmetry). A weak peak could be related with the nonvariation of the apex phonon energy with temperature for the compounds with  $x \leq 0.17$ . The decrease of the energy of this mode with temperature for the  $x=0.24$  sample would imply the absence of the shorter  $\text{Cu-O}_z$  bond in the overdoped region. Also, the asymmetry of the  $A_g$  apex phonon may originate from doping induced local lattice distortions and the second phonon peak. A correlation has already been established at room temperature between the doping dependence of the asymmetry of this phonon (as observed in the  $zz$  polarization) and the relative dependence of  $T_c$ .<sup>6</sup> As can be seen in Fig. 11 a similar correlation between the apex phonon asymmetry and  $T_c$  exists at the lowest temperatures studied. For the  $xx$ -polarization spectra (Fig. 2) the asymmetry of the apex mode is even more pronounced. For  $x=0.03$  and  $0.24$  there is no asymmetry for all temperatures [Figs. 2(a) and 2(e)], while for the other concentrations the asymmetry of the apex phonon is quite clear.

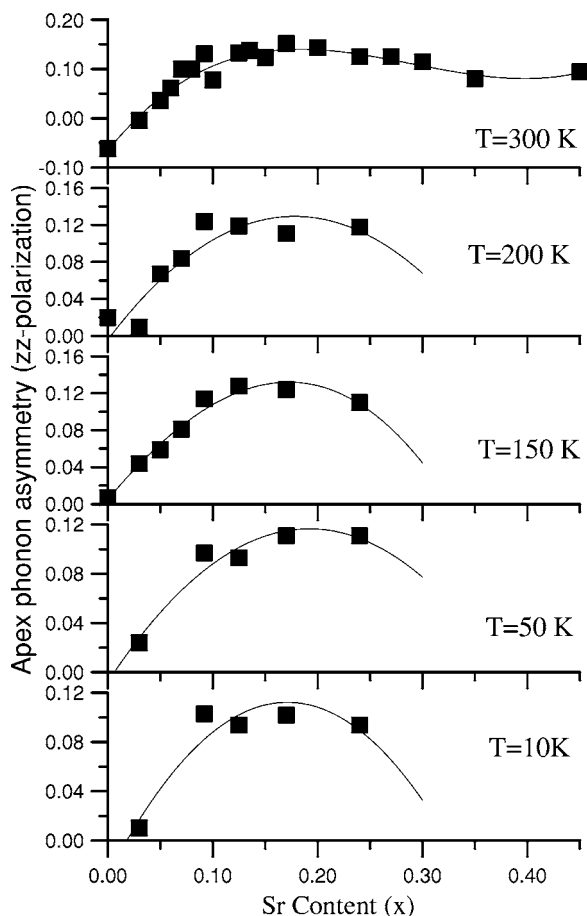


FIG. 11. The dependence of the apex phonon asymmetry on doping, at various temperatures.

For  $x=0.125$  the apex phonon seems to consist at least of another peak at the high-energy side. This critical concentration corresponds to the plateau in the  $T_c$ .

It is known that, at room temperature, the relative intensity of the two strong  $A_g$  phonons varies with doping in a similar way as  $T_c$ .<sup>6</sup> According to the low-temperature data, the relative intensity  $La/apex$  as a function of Sr content reaches a maximum value in the optimally doped region for all temperatures studied (Fig. 12). The substitution of  $Sr^{2+}$  for  $La^{3+}$  in LSCO adds holes to the compound from the La/Sr sites, with the superconductivity appearing when the carrier concentration at the  $CuO_2$  planes exceeds a limit. The small intensity of the La/Sr  $A_g$  phonon for  $x \leq 0.03$  in Fig. 12 can be attributed to the local screening of the light due to the high concentration of carriers at these sites. By increasing the amount of doping, the holes at the La/Sr sites are expected to move to the  $CuO_2$  planes reducing the screening effect and, consequently, increasing the La/Sr phonon intensity. With the further increase of doping above optimal the La/apex relative intensity seems to decrease again, but at much less rate than the initial increase for  $x=0.0-0.03$  (Fig. 12). It is possible that after the optimal doping the additional carriers can no longer move preferentially to the  $CuO_2$  planes screening equally all phonons.

In the  $xx$ - $yy$  scattering polarization and for doping concentrations that the compound is in the tetragonal phase and

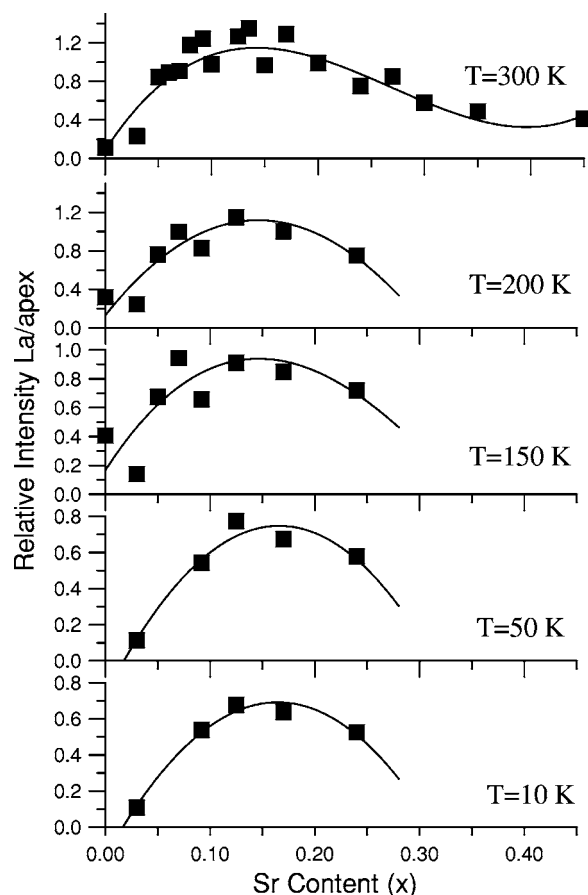


FIG. 12. The dependence of the relative intensity  $La/apex$ , on doping at various temperatures.

superconducting, new symmetry-forbidden modes appear in the Raman spectra (Fig. 2). The space group of the tetragonal structure ( $D_{4h}^{17}$ ) is symorphic with inversion center the Cu site. Since no symmetry lowering has been observed in the crystallographic studies of these materials, the appearance of new modes denotes a local symmetry breaking of the tetragonal structure. This symmetry breaking can be induced by the partial substitution of Sr for La, but then it should be present in any concentration of Sr continuously increasing with the amount of doping, which does not agree with our Raman data [absence of the  $\sim 370\text{-cm}^{-1}$  mode and substantial reduction in the intensity of the  $\sim 150\text{-cm}^{-1}$  for  $x=0.24$ , Fig. 2(e)].

From their energies, the bands at  $\sim 150\text{-cm}^{-1}$  and  $\sim 370\text{-cm}^{-1}$  could be assigned to IR-active phonons. In the  $E||ab$  polarization IR spectra of the tetragonal phase a doubly degenerate  $E_u$  mode exists at  $\sim 140\text{-cm}^{-1}$ ,<sup>2,7</sup> attributed to the vibrations of the apex oxygen atoms parallel to the  $ab$  plane. In the orthorhombic phase the degeneracy is removed and for  $x=0.0$  the  $E_u$  mode splits to one at  $\sim 113\text{-cm}^{-1}$  of  $B_{2u}$  symmetry (vibrations of the  $O_{ap}$  atoms along the  $b$  axis) and another at  $140\text{-cm}^{-1}$  of  $B_{3u}$  symmetry (vibrations of the  $O_{ap}$  atoms along the  $a$  axis).<sup>7</sup> The x-ray diffraction (XRD) measurements have shown,<sup>9</sup> that the  $b$  axis increases substantially in the orthorhombic phase. Therefore, the above splitting depends on the amount of orthorhombic distortion reducing to zero in the tetragonal phase. In the Raman spec-



tra of the orthorhombic phase the  $\sim 150\text{-cm}^{-1}$  band appears at low temperatures as a double or triple peak. The new mode at  $\sim 144\text{ cm}^{-1}$  becomes very narrow and the other one at  $\sim 125\text{ cm}^{-1}$  very broad at low temperatures and doping levels  $x=0.092\text{--}0.17$  [Figs. 2(b)–2(d)]. Besides, there are traces of a peak at  $\sim 170\text{ cm}^{-1}$ , which could correspond to another IR mode<sup>10</sup> [Fig. 2(a)]. The apparent increment of the total width of the  $\sim 150\text{-cm}^{-1}$  band with decreasing temperature for the  $x=0.092\text{--}0.17$  samples (Fig. 8) obviously reflects modifications in the width and intensity of the split modes.

Our data in Fig. 2 indicate that the splitting of the  $\sim 150\text{-cm}^{-1}$  band occurs in the range 200–250 K for  $x=0.092$ , 150–200 K for  $x=0.125$ , and 150–200 K for  $x=0.17$ . In the  $x=0.20$  and  $0.24$  samples, the structural measurements have shown a tetragonal structure at any temperature and the  $\sim 125\text{-cm}^{-1}$  wide mode does not appear to the lowest temperatures [Fig. 2(e)]. In the  $x=0.03$  compound the  $\sim 150\text{-cm}^{-1}$  band is hardly observed [Fig. 2(a)], while for  $x=0.07$  the wide mode at  $\sim 125\text{ cm}^{-1}$  is detected above 125 K. Once the mode at  $\sim 144\text{ cm}^{-1}$  (which can be associated with the IR mode of symmetry vibrations of the  $\text{O}_z$  atoms along the  $a$  axis) appears, it does not vary in energy with decreasing temperature. On the other hand, the mode at  $\sim 125\text{ cm}^{-1}$  (associated with the vibrations of the  $\text{O}_z$  atoms along the  $b$  axis) becomes broader and softens at decreasing temperatures. This could be due to the appearance of another IR mode at lower energy.<sup>10</sup> The Raman spectra with the many new lines that appear at low temperatures are very reminiscent of the formation of stripes in related compounds<sup>11</sup> and fits very well with the findings of Bianconi *et al.*<sup>8</sup> The charge ordering is expected to give rise to the formation of a superlattice, lowering the crystal symmetry and bringing edge phonons to the  $\Gamma$  point. Neutron scattering data on  $\text{LaCuO}_4$  have found a mode of  $A_g$  symmetry at the  $X$  point from the La atoms of similar energy with the  $150\text{-cm}^{-1}$  band.<sup>12</sup> Therefore, the observed multiple modes could also be due to such folded phonons unambiguously defining the formation of stripes.

Concerning the possible assignment of the  $\sim 370\text{-cm}^{-1}$  band to a phonon, it can be seen that in the IR spectra of the tetragonal phase a  $q=0$  mode of  $E_u$  symmetry appears at a similar energy ( $\sim 360\text{ cm}^{-1}$ ).<sup>2,7</sup> This mode has been attributed to the bond bending oxygen vibrations in the  $\text{CuO}_2$  plane and, when the orthorhombic distortion takes place, it splits to one  $B_{2u}$  at  $\sim 353\text{ cm}^{-1}$  and another  $B_{3u}$  mode at  $364\text{ cm}^{-1}$ .<sup>7</sup> Such splitting is not obvious in the Raman spectra, but as it is mentioned previously, the  $\sim 370\text{-cm}^{-1}$  band is broad ( $\sim 30\text{ cm}^{-1}$ ) (see Fig. 9) and, also, seems to have some structure in the low-temperature spectra of the orthorhombic phase [Fig. 2(c)]. The fitting of this band with two Lorentzians results in two peaks that differ by  $\sim 5\text{--}15\text{ cm}^{-1}$ , which agrees with the splitting of the two IR-active modes. Thus, the  $\sim 370\text{ cm}^{-1}$  band could be another IR-active mode that appears in the  $xx$ - $yy$  Raman spectra because of the symmetry breaking. It should be noted that the largest splitting ( $\sim 15\text{ cm}^{-1}$ ) of the  $\sim 370\text{-cm}^{-1}$  band is observed for the underdoped compound ( $x=0.03$ ) at low temperatures, the main reason being the large value of orthorhombicity, which makes the  $b$  axis much larger than the  $a$  axis for this sample.<sup>6,9</sup> The energy of the  $B_{2u}$  vibrations of the  $\text{Cu-O}_{xy}$

bond along the  $b$  axis is expected to be lower than the energy of the  $B_{3u}$  vibrations along the  $a$  axis. Also, the average softening of the total band at  $\sim 370\text{ cm}^{-1}$  with decreasing temperature that has been observed for the  $x=0.03$  sample (see Fig. 9) could be due to a decrease of the energy of the  $B_{2u}$  mode, since the difference between the  $b$  and  $a$  axes increases with decreasing temperature.<sup>9</sup> The latter can also explain the increase of the bandwidth for temperatures below  $\sim 50\text{ K}$  compared with other concentrations. If we assume the formation of stripes and the folding of the Brillouin zone, an edge phonon that could be related with the  $\sim 370\text{-cm}^{-1}$  band would be an  $X$  point mode of similar energy related with the apical oxygen.<sup>12</sup>

The mode at  $\sim 370\text{ cm}^{-1}$  gains intensity together with the broadband at  $\sim 280\text{ cm}^{-1}$  and the wide mode at  $\sim 125\text{ cm}^{-1}$ , which appear mainly at low temperatures (Fig. 2). In previous IR studies there is a weak  $B_{3u}$  phonon at  $\sim 270\text{ cm}^{-1}$  (Refs. 2 and 7) attributed to the vibrations of the Cu atoms in the  $ab$  plane.<sup>7</sup> The broadband at  $\sim 280\text{ cm}^{-1}$  has not been observed in the IR spectra of the doped  $\text{La}_{2-x}\text{Sr}_x\text{CuO}_4$  compounds.<sup>2,7,13</sup> In our compounds this band does not appear in the Raman spectra of the underdoped  $x=0.03$  concentration even at very low temperatures [Fig. 2(a)]. It shows up with increasing Sr concentration and appears even in the high-temperature spectra of the tetragonal phase of the  $x=0.07, 0.092, 0.125,$  and  $0.17$  samples. For the overdoped compounds  $x=0.20$  and  $0.24$ , which are expected to be tetragonal at any temperature, this band is absent to the lowest temperature studied [Fig. 2(e)]. Based on its behavior, it is not possible to assign the very broad  $\sim 280\text{-cm}^{-1}$  band to a specific IR mode activated in the Raman spectra from the breaking of symmetry. McQueeney *et al.* based on inelastic neutron scattering of  $\text{La}_{2-x}\text{Sr}_x\text{CuO}_4$  ( $0.0 \leq x \leq 0.15$ ) at 10 K (orthorhombic phase) have reported a systematic development of anomalous phonon bands near the doping that induces metal to insulator phase transition.<sup>14</sup> From their phonon density of states (PDOS) data, it can be seen that the metal-insulator transition affects the low-energy region, where a band near 30 meV develops close in energy to the  $280\text{-cm}^{-1}$  band that appears in the Raman spectra. Also, the intensity of  $\sim 30\text{ meV}$  is maximized for optimally doped samples, just like the  $280\text{-cm}^{-1}$  mode. Inelastic neutron scattering measurements showed that the  $\sim 30\text{-MeV}$  band is not caused by electrostatic impurity effects from Sr substitution.<sup>15</sup> This band has not been observed in any of the Raman measurements performed on samples with  $x=0\text{--}0.03$  and becomes obvious for higher doping levels. Since the broadband at  $\sim 280\text{ cm}^{-1}$  always appears together with the splitting of the  $\sim 150\text{ cm}^{-1}$  and the wide mode at  $\sim 125\text{ cm}^{-1}$ , and its energy fits well with the combination energies of the two modes at  $\sim 125\text{ cm}^{-1}$  and the  $\sim 144\text{ cm}^{-1}$ , it is possible to be related with a peak in the PDOS. Its appearance mainly at low temperatures whenever the multiple modes around  $150\text{ cm}^{-1}$  develop could also indicate that it might originate from quasiparticle scattering, which in the Raman spectra would create such a high-energy peak.<sup>11</sup>

Finally we examine the dependence of the relative intensity of the  $\sim 150\text{-}, 370\text{-},$  and  $280\text{-cm}^{-1}$  bands over the intensity of the apex phonon at various temperatures. It is already

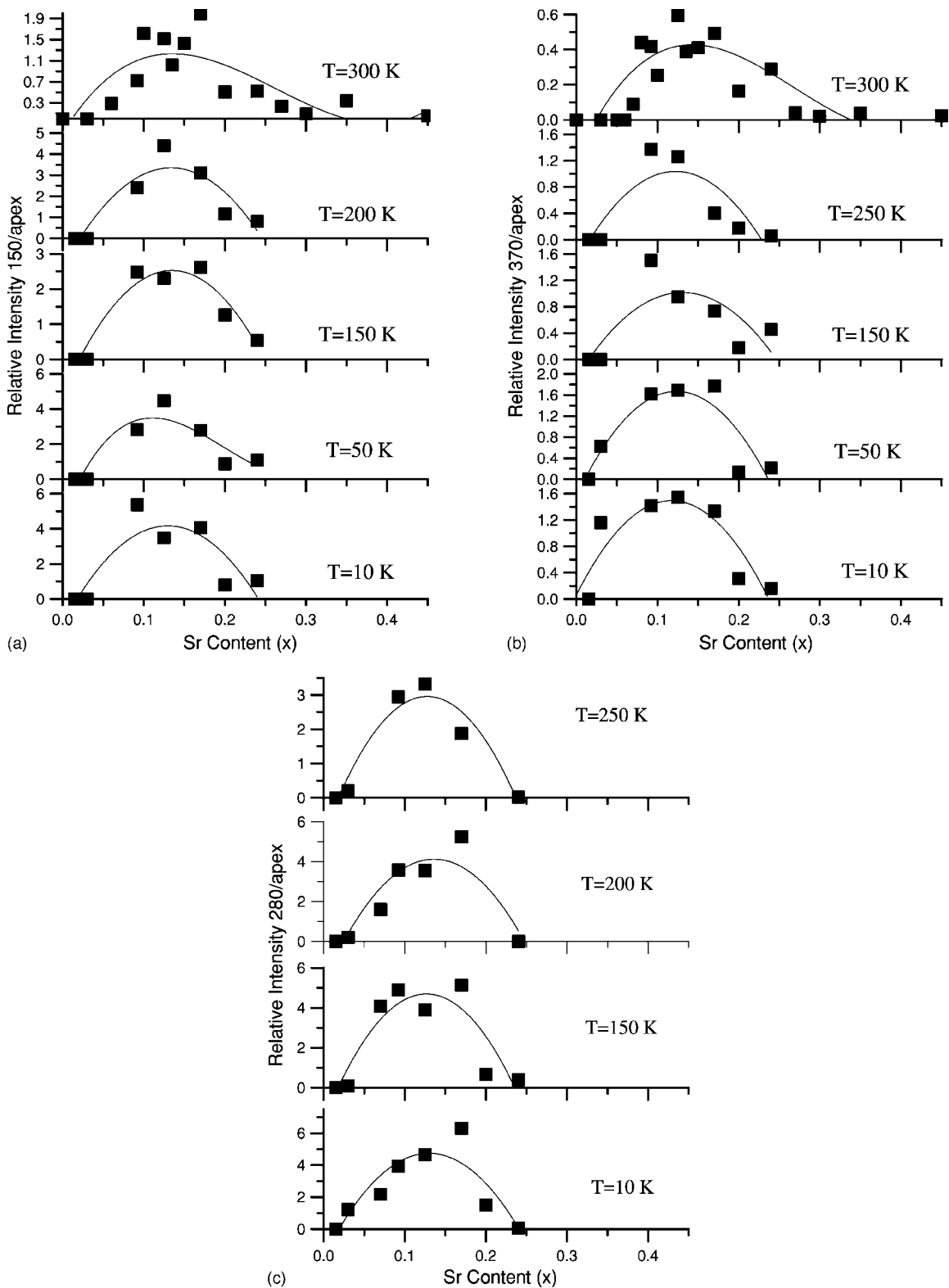


FIG. 13. The dependence of the relative intensities: (a)  $150 \text{ cm}^{-1}/\text{apex}$ , (b)  $370 \text{ cm}^{-1}/\text{apex}$ , and (c)  $280 \text{ cm}^{-1}/\text{apex}$  on doping at various temperatures.

known that there is an apparent correlation of the intensity of the  $\sim 150\text{-cm}^{-1}$  peak with the variation of the superconducting transition temperature  $T_c$  with Sr content.<sup>6</sup> Figure 13 shows the variation of the above mode intensities at various

temperatures (concerning the  $\sim 280\text{-cm}^{-1}$  band the room-temperature data are not included, since this peak has been observed systematically only in the low-temperature spectra). It can be easily seen that the above-mentioned correla-

tion with  $T_c$  persists even at the lowest temperature studied (10 K). From the above results, it can be seen that these intensities mainly depend on the amount of doping and the local lattice distortions induced by doping. Another important effect is the temperature where the broadband at  $\sim 280\text{ cm}^{-1}$  and the splitting of the band at  $\sim 150\text{ cm}^{-1}$  appear (Fig. 2), which varies with doping; it vanishes for  $x < 0.05$  or  $x \geq 0.20$  and shows a maximum around optimal doping.

As is already mentioned above, Bianconi *et al.* have proposed the existence of charge stripes in the optimally doped LSCO, supporting the “two-component” model, where, at optimum doping with 0.2 hole/Cu sites, a first component with hole density  $\delta_i \sim 0.16$  coexists with another component of impurity states with  $\delta_i \sim 0.04$ , spatially separated in two different types of stripes forming a superlattice of quantum wires.<sup>8</sup> It is known that charge stripes break translational (perpendicular to the stripes) and rotational symmetry.<sup>16</sup> The appearance of the above-mentioned modes in the Raman spectra seems to be induced by a symmetry breaking.

On the other hand, it was suggested that the formation of Jahn-Teller real-space pairing can induce a local breaking of symmetry and the appearance of symmetry-forbidden modes in the Raman spectra.<sup>17</sup> The formation of such extended polaron complexes is related with stripes, and it has a doping dependence that resembles the variations observed—i.e., the splitting of the  $\sim 150\text{-cm}^{-1}$  band and the appearance of the broad peak at  $\sim 280\text{ cm}^{-1}$  in the doping range  $0.20 > x > 0.03$ . It seems likely that below a certain temperature the preformed polarons create a long-range order in one direction only and the modes split into a narrowband and a broadband.<sup>11,17</sup> One cannot exclude also the possibility that spin stripes are formed, which break the spin-rotational and time-reversal invariance<sup>16</sup> and coexist with a charge order.<sup>18</sup>

## CONCLUSIONS

In this work it is shown that the  $A_g$  mode at  $\sim 100\text{ cm}^{-1}$  shows a classical soft-mode behavior even for high Sr-doped compounds (up to  $x=0.17$ ), supporting its correlation with the LTO  $\rightarrow$  HTT transition for the Sr contents studied. Also,

the mode at  $\sim 270\text{ cm}^{-1}$  of  $A_g$  symmetry due to vibrations of the plane oxygens along the  $c$  axis correlates with the structural phase transition since it appears only in the spectra of the orthorhombic phase. Further, the energy of this mode varies with temperature contrary to the results of previous works.

The low-temperature measurements have shown that the behavior of the energy and the asymmetry of the apex phonon should be due to local lattice distortions, which are doping induced. The modification of the relative intensity of the La/Sr and the apex phonons seems to be correlated with the carrier concentration on the  $\text{CuO}_2$  planes and consequently with the superconducting transition temperature.

The bands at  $\sim 150$  and  $370\text{ cm}^{-1}$  that appear in the  $xx$ - $yy$  polarization spectra are related to a symmetry breaking that occurs at temperatures that scale with  $T_c$ . The first band splits into at least two modes from which one is very narrow and the other very wide and the spectra are reminiscent of those obtained from the formation of stripes. Another broadband was observed in the  $xx$ - $yy$  polarization spectra at  $\sim 280\text{ cm}^{-1}$ , which appears to scale with the  $T_c$  dependence on doping. This is probably due to a peak in the phonon density of states or to quasiparticle scattering. Moreover, the correlation of the relative intensity of the bands at  $\sim 150$  and  $370\text{ cm}^{-1}$  with the Sr concentration for maximum  $T_c$  that was found at room temperature seems to persist at the lowest temperature studied. A similar connection exists between the intensity of the  $\sim 280\text{-cm}^{-1}$  band and the doping. All these results can be attributed to the formation of stripes at temperatures well above the transition temperature and for doping levels where the compound is superconducting.

## ACKNOWLEDGMENTS

The team from NTUA expresses its appreciation to the Greek Ministry of Education for financial support through the project Pythagoras I, cofunded by the European Social Fund (75%) and Greek National Resources (25%). C.P. and the work in Cambridge were supported by the Royal Society. We thank J. Cooper for providing some of the samples studied. Critical remarks by D. Mihailovic are also appreciated.

<sup>1</sup>B. Keimer, N. Belk, R. J. Birgeneau, A. Cassanho, C. Y. Chen, M. Greven, M. A. Kastner, A. Aharony, Y. Endoh, R. W. Erwin, and G. Shirane, *Phys. Rev. B* **46**, 14034 (1992).

<sup>2</sup>S. Sugai, *Phys. Rev. B* **39**, 4306 (1989); S. Sugai *et al.*, *Solid State Commun.* **76**, 371 (1990).

<sup>3</sup>W. H. Weber, C. R. Peters, and E. M. Logothetis, *J. Opt. Soc. Am. B* **6**, 455 (1989).

<sup>4</sup>G. Burns, G. V. Chandrashekar, F. H. Dacol, and M. W. Shafer, *Solid State Commun.* **68**, 67 (1988).

<sup>5</sup>R. J. Birgeneau, C. Y. Chen, D. R. Gabbe, H. P. Jenssen, M. A. Kastner, C. J. Peters, P. J. Picone, T. Thio, T. R. Thurston, H. L. Tuller, J. D. Axe, P. Boni, and G. Shirane, *Phys. Rev. Lett.* **59**, 1329 (1987).

<sup>6</sup>D. Lampakis, D. Palles, E. Liarokapis, C. Panagopoulos, J. R.

Cooper, H. Ehrenberg, and T. Hartmann, *Phys. Rev. B* **62**, 8811 (2000).

<sup>7</sup>A. V. Bazhenov, C. B. Rezchikov, and I. S. Smirnova, *Physica C* **273**, 9 (1996).

<sup>8</sup>A. Bianconi, N. L. Saini, A. Lanzara, M. Missori, T. Rossetti, H. Oyanagi, H. Yamaguchi, K. Oka, and T. Ito, *Phys. Rev. Lett.* **76**, 3412 (1996).

<sup>9</sup>P. G. Radaelli, D. G. Hinks, A. W. Mitchell, B. A. Hunter, J. L. Wagner, B. Dabrowski, K. G. Vandervoort, H. K. Viswanathan, and J. D. Jorgensen, *Phys. Rev. B* **49**, 4163 (1994).

<sup>10</sup>W. J. Padilla, M. Dumm, S. Komiya, Y. Ando, and D. N. Basov, *Phys. Rev. B* **72**, 205101 (2005).

<sup>11</sup>G. Blumberg, M. V. Klein, and S. W. Cheong, *Phys. Rev. Lett.* **80**, 564 (1998).

- <sup>12</sup>L. Pintschovius and W. Reichardt, in *Physical Properties of High Temperature Superconductors*, edited by D. M. Ginsberg (World Scientific, Singapore, 1994), Vol. IV.
- <sup>13</sup>R. T. Collins, Z. Schlesinger, G. V. Chandrashekhar, and M. W. Shafer, Phys. Rev. B **39**, 2251 (1989).
- <sup>14</sup>R. J. McQueeney, J. L. Sarrao, P. G. Pagliuso, P. W. Stephens, and R. Osborn, Phys. Rev. Lett. **87**, 077001 (2001).
- <sup>15</sup>R. J. McQueeney, J. L. Sarrao, and R. Osborn, Phys. Rev. B **60**, 80 (1999).
- <sup>16</sup>S. A. Kivelson, I. P. Bindloss, E. Fradkin, V. Oganesyan, J. M. Tranquada, A. Kapitulnik, and C. Howard, Rev. Mod. Phys. **75**, 1201 (2003).
- <sup>17</sup>V. V. Kabanov and D. Mihailovic, Phys. Rev. B **65**, 212508 (2002).
- <sup>18</sup>O. Zachar, S. A. Kivelson, and V. J. Emery, Phys. Rev. B **57**, 1422 (1998).